PHYSICAL REVIEW C VOLUME 50, NUMBER 1 JULY 1994

$^2H(\gamma,p)n$ cross section between 20 and 440 MeV

D. A. Jenkins
Physics Department, Virginia Polytechnic Institute and State University, Blacksburg, Virginia 24061

P. T. Debevec
Nuclear Physics Laboratory and Department of Physics, University of Illinois at Urbana-Champaign, Champaign, Illinois 61820

P. D. Harty
Department of Physics and Astronomy, University of Glasgow, Glasgow, Scotland G12 8QQ
(Received 18 November 1993)

Measured total and differential cross sections for deuteron photodisintegration at energies from 20 to 440 MeV are compared to a phenomenological function. The function attempts to represent the coefficients for a Legendre expansion of the differential cross section. The comparison is made by varying parameters in the function to obtain a best fit, in both energy and angle, to the data. The normalization of each data set is allowed to vary according to the quoted systematic error except for data from experiments with bremsstrahlung beams for which the normalization is allowed to vary freely. The analysis included 1615 data from 210 data sets. Measurements of the inverse capture reaction are included by using detailed balance. After rejecting inconsistent data points, we obtain a $\chi^2_{\rm red}$ of 2.0, which indicates the level of consistency in the database and the agreement between the function and the data. The phenomenological function is used as a representation of the data for comparison to a theoretical model.

PACS number(s): 25.10.+s, 25.20.−x

I. INTRODUCTION

A simple phenomenological function has been proposed by Thorlacius and Fearing [1] to fit the total and differential cross sections for deuteron photodisintegration. Rossi *et al.* [2] used this function to fit data in the energy range from 20 to 440 MeV. By fitting the entire database to a function of both energy and angle, they sought to avoid error introduced when parameters for the angular distribution are first derived from the data and then fitted to find their energy dependence. Their technique allows for the inclusion of data sets which are not sufficiently complete to permit an angular analysis. The method produces an interpolation equation which can serve as a check of consistency between experiments and as a comparison of experiment with theory. They obtained a $\chi^2_{\rm red}$ (χ^2/degree of freedom) of 0.9, indicating very good agreement between the data and the phenomenological function. However their analysis used a dubious treatment of systematic errors in the experimental data. We have redone the fit while distinguishing between statistical and systematic errors.

The differential cross section in the center-of-mass (c.m.) frame is represented by the usual Legendre polynomial expansion, to fourth order:

$$\frac{d\sigma}{d\Omega} = \sum_{l=0}^{4} A_l(E_\gamma)P_l(\cos\theta), \qquad (1)$$

where θ is the c.m. angle between the incoming photon and outgoing proton. The energy dependence of the A_0 coefficient was fitted with the phenomenological form:

$$A_0(E_\gamma) = C_1 e^{C_2 E_\gamma} + C_3 e^{C_4 E_\gamma} + \frac{C_5 + C_6 E_\gamma}{1 + C_8(E_\gamma - C_7)^2}, \qquad (2)$$

where C_{1-8} are parameters in the fit. The higher-order coefficients A_1, A_2, A_3, and A_4 were fitted using only C_{1-4}, i.e., the first two terms in Eq. (2).

The fit obtained by Rossi *et al.* [2] to the photodisintegration data was done in four steps. (1) Each angular distribution with at least five measured angles (their Refs. [1–17,19,21,23–26]) was fitted to Eq. (1) with the A_4 coefficient set to zero. (2) The A_0 coefficients determined from step (1) for the experiments which had used monoenergetic photons (from Bonn and Frascati, their Refs. [19,21,23, 24]) and a total cross section measurement (from Frascati, their Ref. [22]) were fitted to Eq. (2) to obtain an interpolation equation for A_0. The A_0 coefficient for this group of data was called $A_{0m}(E_\gamma)$. [Even though Ref. [20] used monoenergetic photons, it was excluded from the fit because only four angles were measured. See step (5) below.] (3) The interpolation formula was then used to calculate an A_0 corresponding to the energy of each data set of step (1), and these data sets were then renormalized so each A_0 agreed with the interpolation equation. (4) The renormalized data of step (3) and the data of three other experiments (Refs.

[25, 26], which also had used monoenergetic photons but were as yet unpublished, and Ref. [33], a measurement at 0°) were fitted to obtain the parameters $C_1 - C_8$ of A_0 and $C_1 - C_4$ of A_l ($l = 1-4$). (5) Rossi *et al.* state that they calculated $\chi^2_{\rm red}$ with respect to all the monochromatic photon data (presumably their Refs. [19–26], with Ref. [20] now included) plus three radiative capture experiments (their Refs. [28–30]) and obtained a value of 0.9. The authors concluded that they had obtained a good fit to the data.

The procedure of Rossi *et al.* is well motivated because the data obtained with monoenergetic photon beams are more reliable than the data obtained with bremsstrahlung. However the method does not correctly differentiate between statistical and systematic errors. Since the data are renormalized and thus correlated, the significance of the χ^2 comparison is lost. We prefer to refit the data using a scheme for χ^2 minimization which simultaneously accounts for the statistical and systematic errors in each data set. We examined the data sets and rejected grossly inconsistent measurements which could bias the final result.

II. PRESENT WORK

For photodisintegration reactions, systematic errors are mainly errors of normalization and represent a correlated uncertainty in the measured values of the data sets. To account for systematic errors, the value of χ^2 for each data set was calculated using the definition of χ^2 introduced by Arndt and MacGregor [3]:

$$\chi^2 = \sum_{i=1} \left(\frac{N\sigma_i^{\rm th} - \sigma_i^{\rm expt}}{\epsilon_i} \right)^2 + \left(\frac{N-1}{\epsilon_N} \right)^2 , \qquad (3)$$

where $\sigma_i^{\rm th}$ is the cross section calculated from the phenomenological function for each data point, $\sigma_i^{\rm expt}$ is the experimental cross section for that point, ϵ_i is the statistical error, ϵ_N is the normalization uncertainty, and N is the normalization constant. The second term of Eq. (3) is introduced to include the contribution to χ^2 of the normalization uncertainty. For each data set, the value of N is found by minimizing χ^2 of Eq. (3):

$$N = \frac{1 + \epsilon_N^2 \sum_{i=1} \sigma_i^{\rm th} \sigma_i^{\rm expt} / \epsilon_i^2}{1 + \epsilon_N^2 \sum_{i=1} \left(\sigma_i^{\rm th} / \epsilon_i \right)^2} . \qquad (4)$$

If either $N = 1$ or the normalization uncertainty is very large, the second term of Eq. (3) does not make a significant contribution to χ^2. Summing the χ^2 for each data set in the database gives a total χ^2 which is then minimized by varying the C coefficients of Eq. (2).

A data set can be one of several types of measurements. Total cross sections reported in a publication are considered one data set. For these data sets the summations in Eqs. (3) and (4) include all data reported in that publication. Angular distributions reported at different energies are considered as different data sets, except for tagged experiments for which the summations in Eqs. (3) and (4) include all energies and angles. With excitation measurements, in which the cross section is measured for various energies over a range of fixed angles, each angle is regarded as defining a different data set.

III. CALCULATION

The data sets include measurements with bremsstrahlung beams [4–23], tagged beams [24–29], laser backscatter [30–32], positron annihilation [33,34], and neutron capture [35–42], covering the energy range 20–440 MeV. The data are essentially the same as used by Rossi *et al.*, but with the addition of seven sets of recently published data. As stated by Rossi, experiments with bremsstrahlung beams have tended to underestimate the systematic errors. For this reason, we have set ϵ_N in Eq. (2) equal to 100 for all differential cross section data collected with bremsstrahlung beams. With this large value of ϵ_N, the normalization is determined by the value which gives the best fit for that data set to the interpolation equation. Thus the normalization for the bremsstrahlung experiments is determined by the other experiments. N is set equal to 1 for the experiment which combined the statistical and systematic errors to give a total error on each data point [38].

Minimizing χ^2 for the complete database of 210 data sets with 1615 cross-section measurements produced a χ^2 of 5863 or a $\chi^2_{\rm red}$ of 3.7 [43]. We were unable to obtain a fit to C_{44}, so this parameter was set equal to 0. Assuming the interpolation equation gives a good representation of the data, our large χ^2 is due to inconsistencies in the data sets. To reduce these inconsistencies, we then pruned the database by removing 83 data which each had a χ^2 greater than 15. Repeating the minimization process, a χ^2 of 3048 was obtained giving a $\chi^2_{\rm red}$ of 2.0. The parameters corresponding to both fits are given in Table I. Our fit parameters are similar to those found by Rossi *et al.*, but our errors are larger.

A frequency histogram of the χ^2 for each data in the data base is shown in Fig. 1. If the interpolation equa-

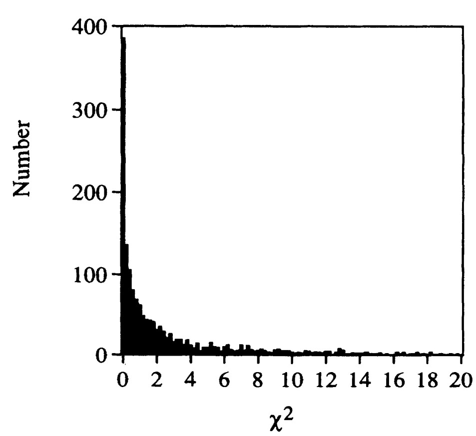

FIG. 1. A frequency histogram of the values of χ^2 for each datum in the database. The pruned database was created by rejecting data with χ^2 greater than 15.

TABLE I. Parameters and errors from χ^2 minimization. The units are the same as given by Rossi *et al.* [2]. They are μb/sr for C_1, C_3, and C_5; GeV^{-1} for C_2 and C_4, μb GeV^{-1}/sr for C_6; GeV for C_7; and GeV^{-2} for C_8. Please see note in text regarding the errors on the parameters.

		Original data set			Pruned data set		
A_0	C_1	14.64	±	0.52	12.17	±	0.35
	C_2	-12.01	±	0.40	-10.70	±	0.36
	C_3	108.7	±	1.5	137.9	±	2.1
	C_4	-59.72	±	0.84	-67.78	±	0.81
	C_5	6.88	±	0.17	6.82	±	0.17
	C_6	-8.48	±	0.51	-8.70	±	0.48
	C_7	0.27975	±	0.00057	0.27921	±	0.00059
	C_8	91.4	±	2.0	91.1	±	2.12
A_1	C_{11}	23.4	±	1.4	32.4	±	2.37
	C_{21}	-52.4	±	2.1	-67.0	±	2.77
	C_{31}	3.282	±	0.077	3.325	±	0.069
	C_{41}	-5.84	±	0.11	-5.81	±	0.10
A_2	C_{12}	-110.8	±	1.7	-131.4	±	2.3
	C_{22}	-55.49	±	0.50	-62.9	±	0.59
	C_{32}	-2.687	±	0.066	-2.585	±	0.065
	C_{42}	-4.432	±	0.11	-4.49	±	0.11
A_3	C_{13}	-27.17	±	2.4	-47.3	±	5.5
	C_{23}	-59.3	±	3.4	-82.7	±	4.5
	C_{33}	-3.48	±	0.25	-3.85	±	0.21
	C_{43}	-11.03	±	0.45	-12.07	±	0.44
A_4	C_{14}	-1.515	±	0.060	-1.48	±	0.15
	C_{24}	-4.822	±	0.64	-2.59	±	0.72
	C_{34}	0.490	±	0.059	0.82	±	0.21

tion is a good approximation to the data, χ^2 should be approximately unity. The large values of χ^2/datum indicate significant discrepancies between the interpolation equation and the data.

The conventional means for assigning an error to a parameter in a χ^2 fit is to find the change in the parameter which produces a change in χ^2 of 1. However this method has little meaning when the database has a large χ^2. For this reason the errors on the parameters in Table I must be regarded with caution. The errors will not give a reliable estimate of the uncertainty in the A_l coefficients of Eq. (2).

IV. COMPARISON WITH DATA

The success of the interpolation equation is illustrated in Figs. 2–4. Figure 2 compares the prediction of Eq. (2), using the parameters obtained from the pruned database given in Table I, with differential cross sections at 67.8 MeV [26]. To account for the normalization factor N of Eq. (4) determined in the fit, the data and errors have been multiplied by 0.95, the reciprocal of N. Comparing the data with the interpolation equation gives a χ^2 of 58 for 47 data points. Figure 3 compares the equation with measurements of the differential cross section at 0°. The data and errors in the figure have been multiplied by the reciprocal of the normalization constant N deter-

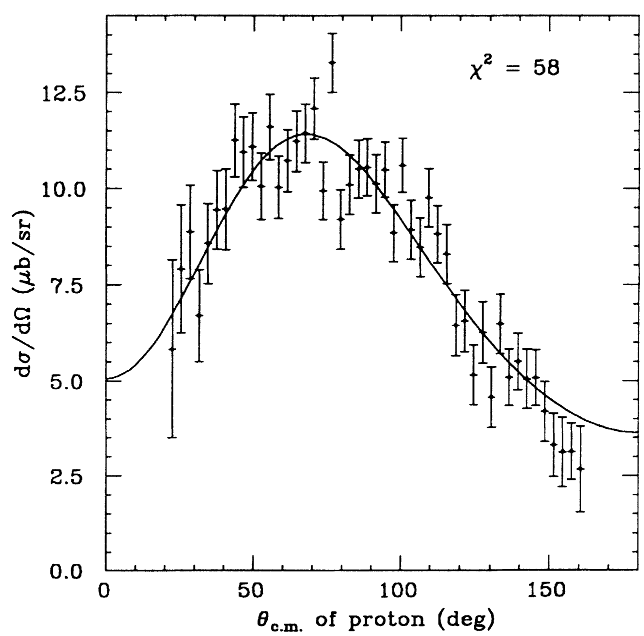

FIG. 2. A comparison of the interpolation equation with differential cross sections at 67.8 MeV [26]. A χ^2 of 58 was calculated for the 47 data points. Statistical errors are shown. The data and errors in the figure have been multiplied by the reciprocal of the normalization constant N determined by Eq. (4).

mined by Eq. (4). Once again the equation gives a good representation of the data. Figure 4 compares the values of the A_l coefficients of Eq. (2) with coefficients derived from the data of Soos *et al.* [20]. The experimental coefficients A_l have been corrected, at each photon energy, by the reciprocal of N found from Eq. (4). In this case systematic differences are seen between the equation and data. The equation is unable to adequately fit the energy dependence of A_1, A_2, and A_3.

The large χ^2 for the total database can also be attributed to inconsistencies between experiments. The experimental situation at 140 MeV has been reviewed by Wallace *et al.* [28]. Comparing recent measurements of the differential cross section at 140 MeV, large differences are found in both the normalization and the angular dependence. Disagreements between different measurements have also been observed by Schmitt *et al.* in their analysis of experiments below 40 MeV [44], and by Jaus *et al.* in their analysis of data up to 200 MeV [45]. Such disagreements between experiments must make a large contribution to χ^2. As shown by Rossi *et al.*, some discrepancies between experiments are removed by renormalizing the bremsstrahlung data. However significant differences remain.

The data used in our calculation of χ^2 is given in Tables II, III, IV, V, and VI. Table II shows the data for the total cross section. Since the total cross section is equal to $4\pi A_0$, these data determine the A_0 parameter of Eq.

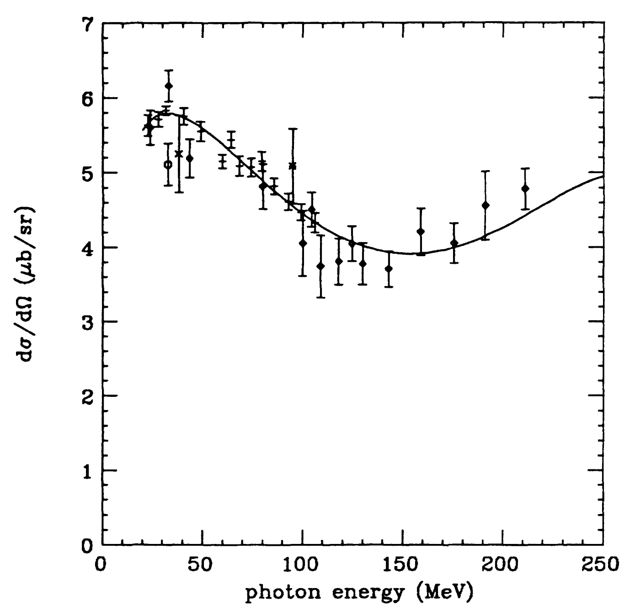

FIG. 3. A comparison of the interpolation equation with differential cross sections at 0°. The data are from Dupont *et al.* [37] (diagonal cross), Hughes *et al.* [14] (diamond), Levi Sandri *et al.* [34] (square), Meyer *et al.* [40] (star), Ninane *et al.* [41] (circle), and Zieger *et al.* [29] (vertical cross). Statistical errors are shown. The data and errors in the figure have been multiplied by the reciprocal of the normalization constant N determined by Eq. (4).

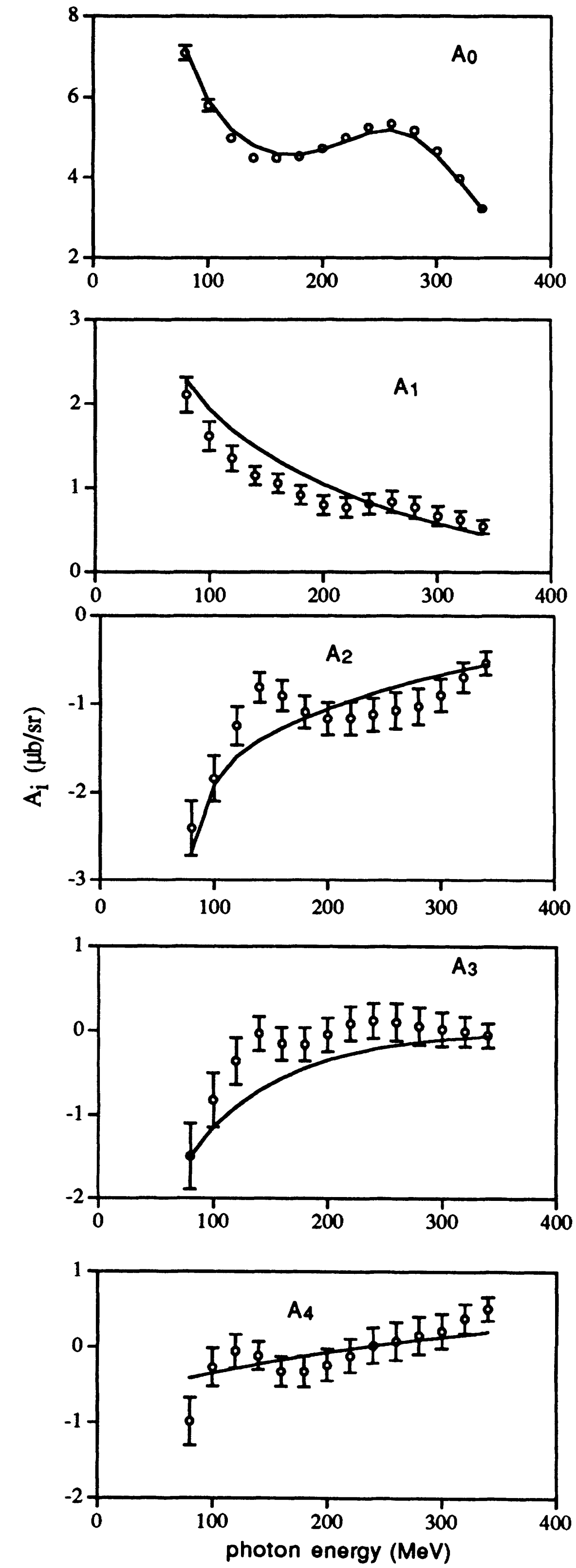

FIG. 4. A comparison of the interpolation equation with the A_l coefficients of Soos *et al.* [20]. The A_l coefficients were calculated from Eq. (2) with the parameters for the pruned data set given in Table I. The errors are statistical only. The data and errors in the figure have been multiplied by the reciprocal of the normalization constant N determined by Eq. (4).

TABLE II. Summary of the total cross-section data in the pruned database. Each experiment is identified by the first two letters of the first author's name and the year of publication. The data were measured with bremsstrahlung beams (brem), neutron capture (n), and a monochromatic beam formed by Compton backscatter with a laser beam (laser). For pruned data sets, the original number of data points is given in parentheses.

Experiment	Energy (MeV)	Beam	No. data points	Syst. error	N	χ^2	χ^2/datum
AH(74) [4]	15–25	brem	2 (3)	0.03	1.00	1.2	0.6
BE(86) [30]	15–74	laser	5 (7)	0.04	1.01	1.6	0.3
BO(79) [35]	20–39	n	7	0.05	0.97	9.4	1.3
AN(69) [8]	220–340	brem	4	0.07	0.93	9.0	2.3

TABLE III. Summary of the differential cross-section data from bremsstrahlung experiments at a fixed energy in the pruned database. For pruned data sets, the original number of data points is given in parentheses.

Experiment	Energy (MeV)	No. data points	N	χ^2	χ^2/datum	Experiment	Energy (MeV)	No. data points	N	χ^2	χ^2/datum
SH(70) [17]	20	4 (5)	0.02	1.4	0.4	KE(56) [15]	105	4	0.78	4.3	1.1
SK(74) [18]	20	19	1.04	32.0	1.7	AL(58) [5]	110	7	1.12	1.9	0.3
HA(53) [13]	20	9	0.00	18.5	2.1	WH(56) [23]	114	4	1.12	4.7	1.2
AL(55) [6]	23	6	0.85	9.3	1.5	KO(67) [16]	120	15 (17)	0.67	47.5	3.2
SH(70) [17]	25	9	0.01	24.8	2.8	SO(92) [20]	120	6	1.01	16.1	2.7
WE(71) [22]	27	7	0.93	13.4	1.9	AL(58) [5]	129	7	0.99	17.2	2.5
AL(55) [6]	27	7	0.88	11.6	1.6	DI(56) [10]	136	4	1.19	4.5	1.1
DE(85) [31]	29	9	0.27	34.5	3.8	KO(67) [16]	140	14 (18)	0.67	32.7	2.3
SH(70) [17]	30	8	0.02	13.3	1.7	BU(68) [9]	140	6	0.72	14.5	2.4
WE(71) [22]	30	7	0.93	9.8	1.4	WH(56) [23]	140	5	0.90	22.7	4.5
AL(55) [6]	34	7	0.91	4.5	0.6	AL(58) [5]	140	7	1.19	16.2	2.3
WE(71) [22]	35	7	0.98	6.2	0.9	SO(92) [20]	140	6 (7)	1.02	19.5	3.2
DE(85) [31]	39	8 (9)	0.44	12.6	1.6	WH(56) [23]	149	5	0.95	1.3	0.3
SH(70) [17]	40	8	0.04	18.8	2.4	DI(56) [10]	150	4 (5)	1.19	7.7	1.9
WE(71) [22]	40	7	1.04	17.9	2.6	KE(56) [15]	155	6	0.86	22.0	3.7
WE(71) [22]	43	7	1.03	15.6	2.2	SO(92) [20]	160	7	1.01	17.3	2.5
AL(55) [6]	43	7	0.95	13.5	1.9	DI(56) [10]	165	6	1.15	8.6	1.4
WE(71) [22]	45	5	1.07	0.9	0.2	KO(67) [16]	180	6 (7)	0.73	25.6	4.3
GA(60) [12]	50	4	1.09	0.9	0.2	BU(68) [9]	180	6	0.79	13.2	2.2
WE(71) [22]	50	4	1.15	5.6	1.4	SO(92) [20]	180	7	1.03	10.1	1.4
AL(58) [5]	54	6	0.85	3.1	0.5	DI(56) [10]	182	6	1.11	8.9	1.5
GA(60) [12]	55	4	1.13	2.3	0.6	WH(56) [23]	194	5	1.38	4.4	0.9
WE(71) [22]	55	4	1.14	2.7	0.7	DI(56) [10]	200	6	1.04	7.0	1.2
SH(70) [17]	55	5	0.07	5.7	1.1	SO(92) [20]	200	7	1.03	11.0	1.6
GA(60) [12]	60	4	1.11	6.9	1.7	KE(56) [15]	205	6	0.94	21.4	3.6
DE(85) [31]	61	5	0.80	19.3	3.9	KO(67) [16]	220	3 (7)	0.84	1.3	0.4
GA(60) [12]	65	4	1.12	4.9	1.1	BU(68) [9]	220	6	0.84	15.4	2.6
WH(56) [23]	65	5	0.98	10.2	2.0	DI(56) [10]	220	6	1.17	3.8	0.6
GA(60) [12]	70	4	1.13	3.9	1.1	WH(56) [23]	220	3	1.06	0.2	0.1
AL(58) [5]	70	6	1.01	8.4	1.4	SO(92) [20]	220	7	1.04	11.8	1.7
SH(70) [17]	70	5	0.10	0.4	0.1	AN(69) [8]	222	15	0.93	5.2	0.3
GA(60) [12]	75	4	1.10	0.5	0.1	SO(69) [19]	240	6	1.02	34.2	5.7
GA(60) [12]	80	4	1.04	0.0	0.0	SO(92) [20]	240	7	1.04	12.7	1.8
WH(56) [23]	80	5	0.87	13.5	2.7	DI(56) [10]	242	6	1.07	7.3	1.2
SO(92) [20]	80	6	0.97	7.7	1.3	WH(56) [23]	248	5	0.92	12.7	2.5
GA(60) [12]	85	4	0.94	0.9	0.2	AN(69) [8]	254	15	0.95	3.9	0.3
AL(58) [5]	88	7	1.13	17.3	2.5	BU(68) [9]	255	6	0.84	16.1	2.7
GA(60) [12]	90	4	0.86	0.8	0.2	KE(56) [15]	255	5 (6)	0.93	11.9	2.4
SH(70) [17]	90	5	0.14	2.7	0.5	KO(67) [16]	260	7	0.83	26.9	3.8
KO(67) [16]	100	15 (18)	0.63	28.6	1.9	SO(69) [19]	260	5 (6)	1.09	7.2	1.4
BU(68) [9]	100	1	0.71	0.0	0.0	SO(92) [20]	260	7	1.03	11.7	1.7
SO(92) [20]	100	6	0.98	7.9	1.3	DI(56) [10]	266	6	1.23	2.9	0.5
WH(56) [23]	105	5	0.96	19.4	3.9	BU(68) [9]	280	6	0.84	15.1	2.5

TABLE III *(Continued).*

Experiment	Energy (MeV)	No. data points	N	χ^2	χ^2/datum	Experiment	Energy (MeV)	No. data points	N	χ^2	χ^2/datum
SO(69) [19]	280	6	1.04	11.6	1.9	SO(92) [20]	320	7	1.03	4.1	0.6
SO(92) [20]	280	7	1.03	10.6	1.5	KO(67) [16]	340	6 (7)	0.85	6.7	1.1
DI(56) [10]	293	6	1.19	8.5	1.4	SO(92) [20]	340	7	1.01	7.6	1.1
KO(67) [16]	300	7	0.90	22.4	3.2	AN(69) [8]	342	15	0.89	10.4	0.7
SO(69) [19]	300	6	1.06	12.4	2.1	KE(56) [15]	355	6	0.83	24.7	4.1
SO(92) [20]	300	7	1.04	7.2	1.0	BU(68) [9]	360	6	0.80	4.6	0.8
AN(69) [8]	302	15	0.91	20.8	1.4	KO(67) [16]	380	7	0.88	23.8	3.4
KE(56) [15]	305	5 (6)	0.91	4.0	0.8	BU(68) [9]	400	6	0.81	25.9	4.3
BU(68) [9]	320	6	0.83	15.6	2.6	KE(56) [15]	405	5 (6)	0.93	2.7	0.5
SO(69) [19]	320	6	1.06	7.6	1.3	KO(67) [16]	420	5 (7)	0.95	15.3	3.1

(2). The table lists, for each experiment, the number of cross-section measurements used in the pruned data. In cases where some data points were removed in pruning, the original number of data points is given in parentheses. The systematic error, which we used as the normalization uncertainty ϵ_N, is quoted as well as the value of N determined by Eq. (4). The χ^2 of the data is also listed. For example, the Ahrens data [4] contained three points of which one had a χ^2 greater than 15 so it was pruned from the database leaving two points for the fit. The data contributed a value of 1.2 to the total χ^2. Table III summarizes the differential cross-section data taken with bremsstrahlung beams at *fixed energy.* Even with a normalization of the data, there are many data sets with χ^2/datum greater than 2.0. The bremsstrahlung differential cross-section data at *fixed angle* is given in Table IV. Once again there are large χ^2/datum for some data sets. The differential cross-sections measured by neutron capture, tagged beams, positron annihilation, and laser beams at fixed energy are given in Table V. Below the threshold for pion production, most of the data give χ^2/datum close to one. However at higher energies there are large χ^2/datum values even after some data were pruned. Differential cross section data for a tagged beam at fixed angle are given in Table VI. There are large χ^2/datum values in these data.

TABLE IV. Summary of the differential cross-section data from bremsstrahlung experiments at fixed angle in the pruned database. For pruned data sets, the original number of data points is given in parentheses.

Experiment	Angle	No. data points	N	χ^2	χ^2/datum
ZI(92) [29]	0	14	1.02	13.6	1.0
HU(76) [14]	0	6	0.94	7.5	1.3
TA(58) [21]	11	3	1.39	0.3	0.1
DO(76) [11]	37	19	1.13	52.7	2.8
DO(77) [11]	37	13	1.07	23.9	1.8
DO(76) [11]	53	17	1.12	39.8	2.3
DO(77) [11]	54	5	1.13	0.7	0.1
DO(77) [11]	66	8	1.11	10.7	1.3
DO(76) [11]	66	15	1.11	61.5	4.1
DO(76) [11]	79	13 (14)	1.05	35.2	2.7
DO(77) [11]	79	8	1.09	3.0	0.4
DO(77) [11]	90	8	1.10	5.1	0.6
DO(76) [11]	90	9 (11)	1.12	18.2	2.0
TA(58) [21]	100	3	1.19	0.1	0.0
DO(76) [11]	102	13 (14)	1.07	50.8	3.9
DO(77) [11]	113	8	1.19	2.2	0.3
DO(76) [11]	114	15	1.07	40.0	2.7
DO(76) [11]	127	11 (12)	1.08	27.4	2.5
DO(77) [11]	141	6	1.28	6.8	1.1
DO(76) [11]	143	9	1.06	26.0	2.9
TA(58) [21]	176	2	1.50	0.0	0.0
AL(83) [7]	180	25 (27)	1.04	60.6	2.4
ZI(92) [29]	180	12	0.98	6.7	0.6

Figure 5 shows the normalization N, calculated by Eq. (4), and the systematic error for each of the data sets listed in Table V. Except for data sets around 150 MeV, most of the sets have a normalization within a standard deviation of one.

V. COMPARISON WITH THEORY

The interpolation equation provides a set of A_i parameters which represent an average of many experiments. These parameters provide a means for comparing experiment with theoretical models. For this comparison, the differential cross sections have been calculated by Leidemann at 20 MeV intervals from 20 to 440 MeV [46]. His model used the Argonne potential with a modified $^1D_2$ partial wave. This is the V_{28} potential cited in the calculation of Leidemann and Arenhövel [47]. We have fitted the differential cross sections of the calculation to Eq. (1) to obtain A_i coefficients which represent the model at each calculated energy.

The comparison between theoretical and experimental values of A_i is given in Fig. 6. It should be noted that the energy range for the comparison includes the region below and above the threshold for pion production. For A_0, theory and experiment are in good agreement below

TABLE V. Summary of the differential cross-section data at a fixed energy in the pruned database for neutron-capture experiments (n), tagged experiments (tag), positron annihilation (e^+), and laser beams with tagged electrons (laser). For pruned data sets, the original number of data points is given in parentheses.

Experiment	Energy	Beam	No. data points	Syst. error	N	χ^2	χ^2/datum
FI(91) [38]	20	n	3	0.000	1.00	4.5	1.5
FI(91) [38]	22	n	3	0.000	1.00	4.2	1.4
FI(91) [38]	27	n	3	0.000	1.00	1.2	0.4
NI(86) [41]	33	n	2	0.037	0.93	4.6	2.3
DU(85) [37]	38	n	2	0.050	1.04	16.3	8.2
KR(88) [27]	54	tag	7	0.030	1.01	9.0	1.3
KR(88) [27]	60	tag	6 (7)	0.030	1.01	7.9	1.3
DE(92) [26]	64	tag	47	0.037	1.05	54.7	1.2
DE(92) [26]	66	tag	47	0.037	1.05	59.9	1.3
DE(92) [26]	68	tag	47	0.037	1.05	58.2	1.2
KR(88) [27]	68	tag	7	0.030	1.01	11.1	1.6
DE(92) [26]	70	tag	47	0.037	1.05	52.1	1.1
KR(88) [27]	88	tag	5 (6)	0.030	1.01	12.2	2.4
CA(86) [36]	92	n	8 (10)	0.062	0.90	12.9	1.6
ME(85) [40]	95	n	11	0.040	0.91	28.9	2.6
LE(89) [34]	100	e^+	2	0.045	1.01	0.8	0.4
DE(86) [33]	100	e^+	4 (5)	0.050	0.92	8.1	2.0
LE(89) [34]	109	e^+	2	0.045	1.03	2.1	1.0
DE(86) [33]	110	e^+	5	0.050	0.95	11.6	2.3
LE(89) [34]	118	e^+	2	0.045	1.04	1.7	0.8
DE(86) [33]	120	e^+	5	0.050	0.96	8.7	1.7
DE(86) [33]	130	e^+	5	0.050	0.86	27.6	5.5
LE(89) [34]	130	e^+	2	0.045	0.97	0.6	0.3
CA(86) [36]	137	n	6 (10)	0.062	0.85	10.4	1.7
WA(91) [28]	139	tag	8 (12)	0.050	0.84	27.9	3.5
DE(86) [33]	140	e^+	5	0.050	0.90	13.6	2.7
LE(89) [34]	143	e^+	3	0.045	0.95	1.4	0.5
DE(86) [33]	150	e^+	5	0.050	0.91	8.8	1.8
WA(91) [28]	152	tag	11 (12)	0.050	0.84	55.8	5.1
LE(89) [34]	159	e^+	3	0.045	0.95	5.2	1.7
DE(86) [33]	160	e^+	5	0.050	0.94	10.3	2.1
DE(86) [33]	170	e^+	5	0.050	0.99	22.9	4.6
LE(89) [34]	176	e^+	3	0.045	0.98	0.4	0.1
DE(86) [33]	180	e^+	5	0.050	1.01	17.6	3.5
MI(92) [32]	187	laser	6 (7)	0.050	0.94	29.6	4.9
HU(87) [39]	187	n	11 (20)	0.150	0.83	51.4	4.7
DE(86) [33]	190	e^+	5	0.050	1.04	5.7	2.0
MI(92) [32]	191	laser	6 (7)	0.050	0.94	30.8	5.1
LE(89) [34]	191	e^+	3	0.045	1.02	1.6	0.5
MI(92) [32]	195	laser	7	0.050	0.94	26.6	3.8
MI(92) [32]	199	laser	7	0.050	0.94	21.1	3.0
DE(86) [33]	200	e^+	5	0.050	1.06	9.5	1.9
AR(84) [24]	200	tag	6 (8)	0.040	1.02	36.1	6.0
MI(92) [32]	203	laser	6 (7)	0.050	0.94	25.3	4.2
MI(92) [32]	207	laser	6 (7)	0.050	0.94	11.6	1.9
DE(86) [33]	210	e^+	5	0.050	1.13	11.4	2.3
MI(92) [32]	211	laser	6 (7)	0.050	0.94	15.9	2.6
LE(89) [34]	211	e^+	3	0.045	1.02	2.6	0.8
MI(92) [32]	214	laser	5 (7)	0.050	0.94	13.5	2.7
MI(92) [32]	218	laser	7	0.050	0.94	21.3	3.0
DE(86) [33]	220	e^+	5	0.050	1.07	3.3	0.7
AR(84) [24]	220	tag	5 (8)	0.040	1.02	15.4	3.0
MI(92) [32]	222	laser	7	0.050	0.94	22.5	3.2
MI(92) [32]	225	laser	6 (7)	0.050	0.94	27.3	4.5
LE(89) [34]	228	e^+	2	0.045	0.98	0.5	0.2
MI(92) [32]	230	laser	7	0.050	0.94	29.7	4.2
DE(86) [33]	230	e^+	5	0.050	1.07	11.9	2.4

TABLE V. (*Continued*).

Experiment	Energy	Beam	No. data points	Syst. error	N	χ^2	χ^2/datum
AR(84) [24]	240	tag	7 (8)	0.040	1.02	23.6	3.4
DE(86) [33]	240	e^+	5	0.050	1.06	17.7	3.5
LE(89) [34]	243	e^+	2	0.045	1.00	0.0	0.0
DE(86) [33]	250	e^+	3 (5)	0.050	1.02	5.1	1.7
AR(84) [24]	260	tag	7 (8)	0.040	1.02	5.8	0.8
AR(84) [24]	280	tag	8	0.040	1.02	19.4	2.4
AR(84) [24]	300	tag	7 (8)	0.040	1.02	24.9	3.6
AR(84) [24]	320	tag	8	0.040	1.02	29.6	3.7
AR(84) [24]	340	tag	5 (8)	0.040	1.02	20.0	4.0
AR(84) [24]	360	tag	8	0.040	1.02	18.1	2.3
AR(84) [24]	380	tag	8	0.040	1.02	5.2	0.6
AR(84) [24]	400	tag	8	0.040	1.02	15.1	1.9
AR(84) [24]	420	tag	8	0.040	1.02	8.1	1.0
AR(84) [24]	440	tag	8	0.040	1.02	14.7	1.8

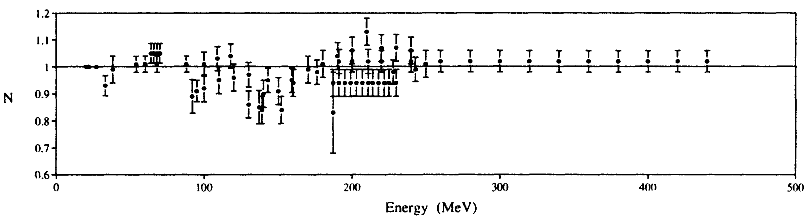

FIG. 5. The calculated normalization N for the data sets measured by neutron capture, tagged beams, positron annihilation and laser beams given in Table V. The systematic error is shown for each data point. The solid line indicates the expected value of 1.

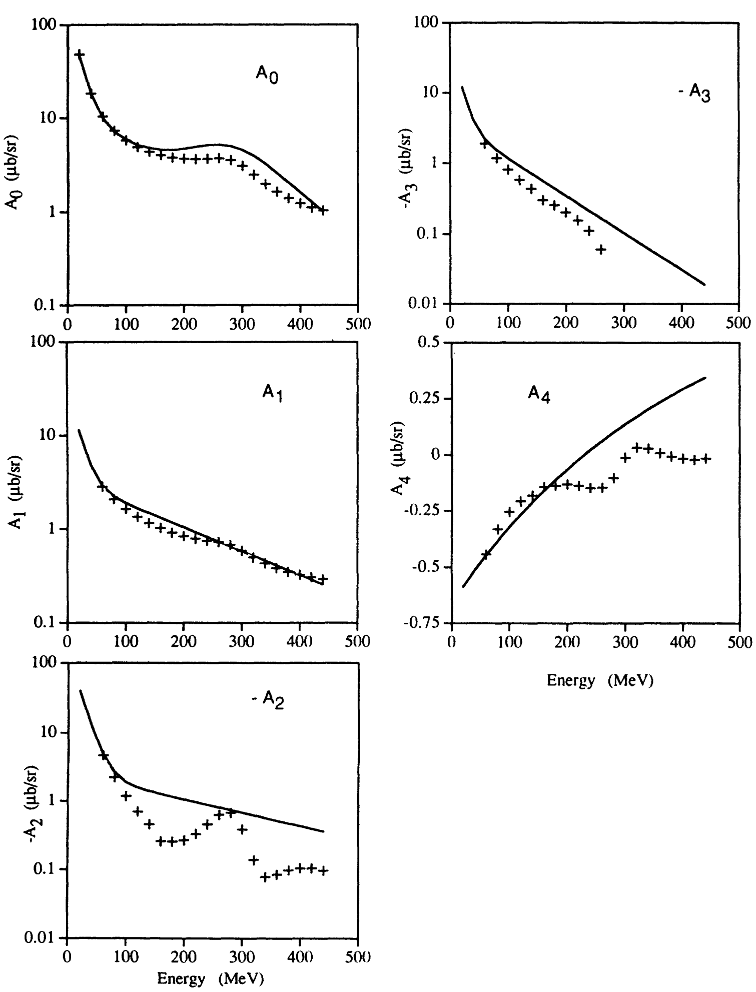

FIG. 6. A comparison of the interpolation equation (solid line) with a theoretical calculation using the potential of Arenhövel and Leidemann (crosses) [47].

TABLE VI. Summary of the differential cross-section data for tagged experiments at a fixed angle in the pruned database. For pruned data sets, the original number of data points is given in parentheses.

Experiment	Angle	No. data points	Syst. error	N	χ^2	χ^2/datum
BA(83) [25]	14.9	8 (9)	0.15	0.91	18.7	2.3
BA(83) [25]	26.1	3 (6)	0.15	0.91	20.2	6.7
BA(83) [25]	28.7	8	0.15	0.91	15.9	2.0
BA(83) [25]	42.1	4	0.15	0.91	33.2	8.3
BA(83) [25]	70.6	4	0.15	0.91	2.7	0.7

120 MeV. The model tends to agree with experiment up to 200 MeV then falls below the experimental values. For A_1, the model falls below experiment between 100 and 240 MeV. Since the values of A_2 and A_3 are negative, the absolute values are plotted in order that they can be compared on a logarithmic scale. For A_2, theory and experiment agree up to 80 MeV, but then theory falls below experiment and shows a strong energy dependence which is not observed in the data. The theoretical predictions for A_3 are less than experiment and change sign as energy increases while the experimental value remains negative. Theoretical values for A_3 are not plotted at high energies where they change sign. The experimental value of A_4 rises more rapidly than theory with increasing energy, but there is fair agreement considering the uncertainties in the measurement of this parameter.

VI. CONCLUSION

The interpolation equation discussed by Rossi *et al.* gives a useful representation of the data. As they show, early disagreements between bremsstrahlung experiments can be reduced by renormalizing the data. However, even then, a large χ^2 is obtained when the proper normalization procedures are used, because of inconsistencies in the data set and the inability of the equation to give a good representation of the data. Accurate measurements of the differential cross section over the full energy range are needed to resolve these conflicts and allow an unambiguous analysis of the data.

The present data are in fair agreement with theory except for the A_2 parameter above 80 MeV and the A_3 parameter at high energies where the theoretical values change sign.

ACKNOWLEDGMENTS

We thank Professor Richard Arndt for his assistance and advice and Professor Winfried Leidemann for his calculation of the differential cross sections. We thank Dr. P. Rossi and Dr. E. De Sanctis for informative correspondence. This work has been supported by the National Science Foundation under Grant Nos. NSF-PHY85-20738, NSF-PHY86-10493, NSF-PHY89-21146, and NSF-PHY91-12528.

[1] A. E. Thorlacius and H. W. Fearing, Phys. Rev. C **33**, 1830 (1986).
[2] P. Rossi, E. De Sanctis, P. Levi Sandri, N. Bianchi, C. Guaraldo, V. Lucherini, V. Muccifora, E. Polli, and A. R. Reolon, Phys. Rev. C **40**, 2412 (1989).
[3] R. A. Arndt and M. H. MacGregor, *Methods in Computational Physics* (Academic, New York, 1966), Vol. 6, pp. 253–296.
[4] J. Ahrens, H. B. Eppler, H. Gimm, M. Kröning, P. Riehn, H. Wäffler, A. Zieger, and B. Ziegler, Phys. Lett. **52B**, 49 (1974).
[5] Iu. A. Aleksandrov, N. B. Delone, L. I. Slovokhotov, G. A. Sokol, and L. N. Shtarkov, Zh. Eksp. Teor. Fiz. **33**, 614 (1958) [Sov. Phys. JETP **6** , 472 (1958)].
[6] L. Allen, Jr., Phys. Rev. **98**, 705 (1955).
[7] K. H. Althoff *et al.*, Z. Phys. C **21**, 149 (1983).
[8] R. L. Anderson, R. Prepost, and B. H. Wiik, Phys. Rev. Lett. **22**, 651 (1969).
[9] J. Buon, V. Gracco, J. Lefrancois, P. Lehmann, B. Merkel, and Ph. Roy, Phys. Lett. **26B**, 595 (1968).
[10] D. R. Dixon and K. C. Bandtel, Phys. Rev. **104**, 1730 (1956).
[11] P. Dougan, T. Kivikas, K. Lugnér, V. Ramsay, and W. Stiefler, Z. Phys. A **276**, 55 (1976); P. Dougan, V. Ramsay, and W. Stiefler, *ibid.* **280**, 341 (1977).
[12] J. A. Galey, Phys. Rev. **117**, 763 (1960).
[13] J. Halpern and E. V. Weinstock, Phys. Rev. **91**, 934 (1953).
[14] R. J. Hughes, A. Zieger, H. Waffler, and B. Ziegler, Nucl. Phys. **A267**, 329 (1976).
[15] J. C. Keck and A. V. Tollestrup, Phys. Rev. **101**, 360 (1956).
[16] R. Kose, W. Paul, K. Stockhorst, and K. H. Kissler, Z. Phys. **202**, 364 (1967).
[17] Y. M. Shin, J. A. Rawlins, W. Buss, and A. O. Evwaraye, Nucl. Phys. **A154**, 482 (1970).
[18] D. M. Skopik, Y. M. Shin, M. C. Phenneger, and J. J. Murphy, Phys. Rev. C **9**, 531 (1974).
[19] D. I. Sober, D. G. Cassel, A. J. Sadoff, K. W. Chen, and P. A. Crean, Phys. Rev. Lett. **22**, 430 (1969).
[20] T. Soos *et al.* (unpublished).
[21] C. A. Tatro, T. R. Palfrey, Jr., R. M. Whaley, and R. O. Haxby, Phys. Rev. **112**, 932 (1958).
[22] B. Weissman and H. L. Schultz, Nucl. Phys. **A174**, 129 (1971).
[23] E. A. Whalin, B. D. Schriever, and A. O. Hanson, Phys. Rev. **101**, 377 (1956).
[24] J. Arends, H. J. Gassen, A. Hegerath, B. Mecking, G. Nöldeke, P. Prenzel, T. Reichelt, A. Voswinkel, and W. W. Sapp, Nucl. Phys. **A412**, 509 (1984).
[25] K. Baba *et al.*, Phys. Rev. C **28**, 286 (1983).
[26] P. T. Debevec, P. D. Harty, J. E. Knott, D. A. Jenkins,

and R. T. Jones, Phys. Rev. C **45**, 904 (1992).
[27] K.-H. Krause, J. Sobolewski, J. Ahrens, J. M. Henneberg, and B. Ziegler, Nucl. Phys. **A549**, 387 (1992).
[28] P. A. Wallace *et al.*, Nucl. Phys. **A532**, 617 (1991).
[29] A. Zieger *et al.*, Phys. Lett. B **285**, 1 (1992); A. Zieger *et al.*, *ibid.* **287**, 51 (1992).
[30] R. Bernabei *et al.*, Phys. Rev. Lett. **57**, 1542 (1986).
[31] M. P. De Pascale *et al.*, Phys. Rev. C **32**, 1830 (1985).
[32] W. K. Mize, Ph.D. thesis, University of South Carolina, 1992.
[33] E. De Sanctis *et al.*, Phys. Rev. C **34**, 413 (1986).
[34] P. Levi Sandri *et al.*, Phys. Rev. C **39**, 1701 (1989).
[35] M. Bosman, A. Bol, J. F. Gilot, P. Leleux, P. Lipnik, and P. Macq, Phys. Lett. **82B**, 212 (1979).
[36] J. M. Cameron *et al.*, Nucl. Phys. **A458**, 637 (1986).
[37] C. Dupont, P. Leleux, P. Lipnik, P. Macq, and A. Ninane, Nucl. Phys. **A445**, 13 (1985).
[38] G. Fink, P. Doll, S. Hauber, M. Haupenthal, H. O. Klages, H. Schieler, F. Smend, and G. D. Wicke, Nucl. Phys. **A530**, 331 (1991).
[39] M. Hugi *et al.*, Nucl. Phys. **A472**, 701 (1987).
[40] H. O. Meyer, J. R. Hall, M. Hugi, H. J. Karwowski, R. E. Pollock, and P. Schwandt, Phys. Rev. C **31**, 309 (1985).
[41] A. Ninane, C. Dupont, P. Leleux, P. Lipnik, and P. Macq, Phys. Rev. C **35**, 402 (1987).
[42] P. Wauters, C. Dupont, P. Leleux, P. Lipnik, P. Macq, A. Ninane, and S. W. Kitwanga, Few Body Syst. **8**, 1 (1990).
[43] The number of degrees of freedom is equal to the number of data points minus the number of free parameters. The number of data points is equal to the number of cross-section measurements plus the number of normalization terms introduced by the second term on the right side of Eq. (3). The number of free parameters is equal to 23 plus the number of normalization terms since the normalization terms were allowed to vary during the fit. Thus the number of degrees of freedom is equal to the number of cross-section measurements minus 23.
[44] K.-M. Schmitt, P. Wilhelm, and H. Arenhövel, Few Body Syst. **10**, 105 (1991).
[45] W. Jaus, D. Bofinger, and W. S. Woolcock (unpublished).
[46] W. Leidemann (private communication).
[47] W. Leidemann and H. Arenhövel, Nucl. Phys. **A465**, 573 (1987).